Intratumoral distribution of YSNSG cyclopeptide in a mouse melanoma model using microdialysis

Florian Slimano, Zoubir Djerada, Juline Guerin, Morad Id Bellouch, Sylvie Brassart-Pasco, Sylvain Dukic

Title page

Intratumoral Distribution of YSNSG Cyclopeptide in a Mouse Melanoma Model using Microdialysis

Florian Slimano[a,b*], Zoubir Djerada[c], Juline Guerin[a], Morad Id Bellouch[a], Sylvie Brassart-Pasco[a], Sylvain Dukic[a,b]

[a]MEDyC Research Unit, UMR CNRS/URCA n°7369, SFR CAP-Santé, Reims University, 51, rue Cognacq-Jay, 51100 Reims

[b]Department of Pharmacy, CHU Reims, Avenue du General Koenig, and Faculty of Pharmacy, Reims University, 51, rue Cognacq-Jay, 51100 Reims

[c]Department of Pharmacology and Toxicology, CHU Reims; Avenue du General Koenig, 51100 Reims and EA3801, SFR CAP-Santé, Faculty of Medicine, Reims University, 51, rue Cognacq-Jay, 51100 Reims

* *Corresponding author:*
Florian Slimano
Faculty of Pharmacy
Reims University
51, rue Cognacq-Jay, 51100 Reims
florian.slimano@univ-reims.fr
Tel: (+33)3.26.91.80.81

ORCID: https://orcid.org/0000-0001-5139-7034

Manuscript: **4,364** words

Abstract: **250** words

Number of Figures: **4**

Number of Tables: **2**

Number of Supplementary file: **1**

Number of references: **39**

Abstract

The YSNSG peptide is a synthetic cyclopeptide targeting $\alpha_v\beta_3$ integrin with antitumor activity. Previous study has determined main pharmacokinetic parameters in plasma and in tissue in healthy animals using microdialysis. First we aim to assess the impact of a 20 mg/kg dosage instead of 10 mg/kg in tumor growth inhibition. Secondly we aim to investigate the YSNSG peptide distribution in two different tumor regions in animals with melanoma. C57BL/6 mice were exposed at Days 8, 10 and 12 after melanoma cells implantation (B16F1) to different dosage of YSNSG peptide or control, respectively (n=10 per group). Data analysis was performed at D16, 20 and 24 with a Nonlinear Mixed-Effects (NLME) approach. For pharmacokinetic study n=8 mice (same disease condition) received YSNSG peptide by intravenous after insertion of two microdialysis probes in central peripheral region of tumor, respectively. Plasma and tissue samples were collected during 2 hours. A non-compartmental analysis was performed to determine main pharmacokinetic parameters. There was a significant tumor growth inhibition in mice receiving 20 mg/kg vs Control ($p<0.02$). Main plasma parameters were half-life elimination 25.8 ± 8.2 min, volume of distribution 11.9 ± 0.4 mL, clearance 19.8 ± 9.4 mL/h and area under the curve 1,173.6 µg.min/mL. Penetration rate of the YSNSG peptide from plasma to tumor tissue were 3.3 ± 2.1% and 3.4 ± 2.7% in central and peripheral, respectively. Contrary to subcutaneous distribution in healthy animals the distribution of the YSNSG peptide into tumoral tissue is low but seems non-heterogeneous between central and peripheral tumor region.

Keywords

Integrin antagonist; melanoma; microdialysis; pharmacokinetic; YSNSG; cyclopeptide; intratumoral distribution

1. Introduction

Tumor microenvironment is a complex environment where cellular and tissue entities interfere (Hanahan et al., 2011). Communication among cells or between cells and basal membrane can promote tumor progression. Specifically, interactions between cancer cells and basal membrane mediated by cellular adhesion molecules like integrin can enhance cellular migration and tumor invasion (Francavilla et al., 2009; Shattil et al., 2010). Consequently, integrin inhibition, especially alpha v beta 3 ($\alpha_v\beta_3$) integrin turns out to be promising in anticancer treatment. Our research group isolated an active sequence [Tyr-Ser-Asn-Ser] that binds $\alpha_v\beta_3$ integrin and designed a cyclopeptide [Tyr-Ser-Asn-Ser-Gly] in order to stabilize the β-turn conformation of the original peptide and to increase its anti-tumor properties. This YSNSG cyclopeptide has shown significant inhibition of tumor growth in vivo and angiogenic activity in melanoma tumor-bearing mice (Thevenard et al., 2006; Thevenard et al., 2010). In order to explore pharmacokinetic parameters we performed the first pharmacokinetic study about YSNSG peptide in healthy Wistar rats, using microdialysis to investigate both subcutaneous and cerebral disposition. The concentration-time profile of YSNSG in plasma showed a bicompartimental decrease with a volume of distribution of 433.7 ± 272.2 mL, an elimination half-life of 2.56 ± 1.52 h and a total clearance of 10.7 ± 6.3 mL/min/kg (Slimano et al., 2017). The area under the curve (AUC) was 1473.19 ± 1054.99 µg.min/mL and the penetration rate of YSNSG in subcutaneous and cerebral tissue (AUC_{ECF} / AUC_{plasma} ratio) were 66.2 ± 21.6% and 3.6 ± 4.7 %, respectively.

This first pharmacokinetic study highlighted that subcutaneous tissue disposition of YSNSG peptide was high and potentially sufficient to a pharmacological effect, which was not the case for cerebral tissue. Moreover, the pharmacokinetic model showed good prediction of subcutaneous YSNSG peptide concentration from plasma compartment. However this *in vivo*

study was performed only on healthy animals and did not take into account the tumor complexity. Intratumoral tissue heterogeneity can lead to a heterogeneous disposition of anticancer drug and drug resistance phenomena (Trédan et al., 2007). This can also limit the predictability of tumor tissue exposition by plasma pharmacokinetic model and consequently anticancer drug response. For example, a recent study about etoposide penetration into the intratumoral tissue (rats with carcinosarcoma Walker-256 tumor) and using two microdialysis probes showed that etoposide plasma concentrations were not a good surrogate for tumoral disposition assessment and they claimed for the importance of knowing intratumoral concentrations to predict drug response (Pigatto et al., 2016). In order to perform a pharmacokinetic study relative to the possible tumor effect on the drug disposition, we first aimed to re-explore the pharmacological active dose of YSNSG peptide in a mice melanoma model. Subsequently and to investigate the possible effect of the intratumoral heterogeneity on the YSNSG peptide disposition, we performed a pharmacokinetic study exploring the penetration rate from plasma to two different intratumoral region of the same melanoma tumor model.

2. Material and Methods

2.1.Ethical information

All procedures performed in studies involving animals were in accordance with the ethical standards of the institution or practice at which the studies were conducted. The study protocol was approved by the Ethics Committee of Animal Experimentation of Reims University (the “comité d’éthique en expérimentation animale de Reims Champagne-Ardenne”; C2EA-56) and by the Ministry of national education, higher education and research (APAFIS#4367-2016030318206226 v2).

2.2.Chemicals

YSNSG cyclopeptide (powder) was obtained from Proteogenix (Schiltigheim, France). Isoflurane (ISOFLO®) was from Centravet (Nancy, France). Saline solution (0.9%) VERSOL® was from Aguettant (Lyon, France). Heparin saline was prepared adding 12,500 IU calcic heparin (Heparine Choay 25,000 IU / 5 mL) in 500 mL saline. All other reagents used in this study were of pharmaceutical analytical grade.

2.3.Cells

B16F1 cells were cultured in RPMI 1640 medium supplemented with 5% fetal bovine serum under a humidified atmosphere of 5% CO_2 in air. Cell number was determined using the Countess Automated cell counter from Thermo Fischer Scientific (Illkirch, France).

2.4.Animals

Female C57Bl/6 mice (25 g in weight; Janvier Labs, Le Genest-Saint-Isle, France) were penned in a controlled environment (temperature: 21 ± 2 °C; relative humidity: 65 ± 15%; alternating natural light/dark cycles). The animals were fed a standardized diet (UAR, Villemoisson on barley, France), and tap water was provided ad libitum. Four groups (n=10) were constituted for tumor growth inhibition experiment: three groups were treated with intraperitoneal YSNSG, 5 mg/kg, 10 mg/kg or 20 mg/kg, respectively, and one group served as control. Eight mice in the control group were re-used for pharmacokinetic experimentation at approximately 24 days after B16F1 cells injection.

2.5.YSNSG dilution and administration

YSNSG peptide reconstitution for intraperitoneal administration was performed by diluting in saline to obtain a concentration of 1 mg/mL from which solutions for i.p. were prepared according to the treatment group. YSNSG peptide reconstitution for intravenous administration was performed by diluting in saline to obtain a concentration of 4 mg/mL from

which injectable volumes of 150 µL maximum were prepared in order to be compatible for retro-orbital bolus administration (Yardeni et al., 2011).

2.6.*In vivo* tumor growth measurement

Suspension of B16F1 cells (250,000 cells in 0.1 mL RPMI 1640 medium) were subcutaneously injected into the left side of anesthetized (isoflurane 1.5-5%) different series of syngenic C57Bl/6 mice. YSNSG intraperitoneal injections were performed at day 8, 10 and 12 (whatever the group: 5 mg/kg, 10 mg/kg and 20 mg/kg). Tumor volume were measured every 3 days from day 8 and determined according to $T_{vol} = A/2 \times B^2$ were A denotes the largest dimension of the tumor and B represents the smallest dimension (Wald et al., 2001). Mice were sacrificed (including control group after pharmacokinetic experiment) when $T_{vol} \geq 2\ cm^3$.

2.7.Growth tumor inhibition analysis

As for repeated measures, the relation between tumor volume (T_{vol}) and time (days) was assessed using nonlinear mixed effect model lme4 version 1.1-19, for R 3.1.4 (The R Foundation for Statistical Computing, http://www.r-project.org) package (Bates et al., 2014). Lme4 modeling is more appropriate, especially for repeated, auto-correlated measures with between-individual or within individual variability. The model best describing individual data was selected and evaluated based on the usual diagnostic plot, precision and information criteria with minimum parameters (to prevent overfitting) (Djerada et al., 2017). The likelihood ratio test (LRT), including the −2 log-likelihood, the Akaike information criterion (AIC) for nested model and the Bayesian information criterion (BIC) for non-nested model, was used to test different hypotheses regarding the final model. The goodness of fit was evaluated with the diagnostic plot produced from the final model: correlation between observed and predicted individual measurements, distributions of pearson residuals as

centered on zero, without systematic bias, no outliers with the minimum and maximum values of standardized residual within [-3, + 3] values, normal distribution with mean = 0 and a constant variance not different from 1, and graphically by mean of QQplot (Djerada et al., 2017). The robustness of the model and the stability of the final parameter were also evaluated using the nonparametric bootstrap procedure (n=1000). For all statistical tests (parametric and non-parametric) the significance level for the first alpha type was 0.05.

2.8.Microdialysis system

The microdialysis system was composed of a syringe infusion pump (Harvard Apparitus, Les Ulis, France) used to infuse the perfusate solution (heparin saline) and two microdialysis probes (per mice); CMA/20 microdialysis probes with membrane length of 10 mm and cutoff of 20 kDa (Phymep, Paris, France). First probe was inserted centrally according to the B16F1 tumor volume and was considered as the "region 1" for the study whereas the second probe was inserted tangentially according to the same B16F1 tumor and was considered as the "region 2" for the study (Fig. 1 and Supplementary file 1).

2.9.Recovery of microdialysis probes

In vitro and in vivo microdialysis probe recoveries of YSNSG were determined based on the reverse dialysis method (Ståhle et al., 1991) [13]. *In vitro* recovery was performed by infusing the microdialysis probe at a rate of 1 µL/min using two different solution containing YSNSG (100 and 400 ng/mL in saline). Thirty-minutes-interval sample dialysates were collected between 30 and 120 minutes (n=4). *In vivo* recovery was individually performed for all mice before pharmacokinetic experiment by infusing both microdialysis probes at a rate of 1 µL/min with a solution containing YSNSG (100 ng/mL in saline). Thirty-minute-interval sample dialysates were collected between 30 and 90 min (n=3) followed by a wash-out period of 30 min with a flow rate of 3 µL/min. *In vitro and in vivo* relative recovery was defined as

the ratio of the concentration difference between the dialysate (C_{dial}) and perfusion fluid (C_{perf}) over the concentration in the perfusion fluid (Eq. (1)) (Scheller and Kolb, 1991).

$$\textit{In vivo} \text{ relative recovery (\%)} = \frac{Cperf - Cdial}{Cperf} \times 100 \quad (1)$$

2.10. Plasma protein binding

To determine the plasma protein binding (PPB) of YSNSG, plasma samples at different time points were pooled to span the entire concentration range. Plasma protein binding was determined using the Centrifree ultrafiltration device with a YM-T Ultracel® membrane (Dutscher SA, Brumath, France). All procedures were performed according to the user's manual. The ultrafiltrate was diluted 10 times with saline before the analysis.

2.11. Pharmacokinetic experimentation

All animals (n=8), first anesthetized with isoflurane (1.5-5%), underwent the intravenous administration (i.v.) of YSNSG at 20 mg/kg. Anesthesia was administered for 120 min by inhalation of isoflurane (induction: 5% and maintenance: 1-1.5%) by means of an isoflurane evaporator (MSS, Harvard Apparatus, France). Animals were ventilated with an oxygen concentrator (Oxyconcentrator, Oxy Life, Minerve, France). During this period the mice where kept at 37 °C with a temperature controller (Mediheat V500VSat, Harvard Apparatus France). The both microdialysis probes previously used for relative recovery were kept during a washout period of 30 min (with a flow rate of 3 µL/min) following which a sample was collected in order to assess that the YSNSG peptide concentration was below the lower limit of quantification. The probes were then perfused with saline at a flow rate of 1 µL/min for 120 min. Blood samples from blood vessel in the tail were taken at the following time intervals: 15, 30, 60, 90 and 120 min. They were then temporarily stored in heparin (0.2 IU)-coated Eppendorf cups before being centrifuged for 10 min at 4000 rpm. The plasma was then

pipetted into clean Eppendorf cups and was stored at -20 °C for subsequent analysis. Dialysates were collected (every 30 min) in vial cups (100 µL) using a refrigerated fraction collector (820 Microsampler, UNIVENTOR) and were stored at -20°C for subsequent analysis. At the end of the experiments, the animals were sacrificed.

2.12. Sample pre-treatment and analysis

YSNSG concentrations were determined by UPLC-MS/MS (Slimano et al., 2017; Djerada et al., 2013) after a 1/100 dilution (with water + 0.1 % (V/V) formic acid) for plasma or 1/10 dilution for dialysates. All compounds (YSNSG and MRFA ([Met-Arg-Phe-Ala]) as the internal standard) were eluted within a 3.5 min run time using a programmed mobile-phase gradient of water/0.1 % (V/V) formic acid and acetonitrile/0.1 % (V/V) formic acid at a flow rate of 0.8 mL/min. Chromatographic separation was achieved using a Waters Acquity HSS T3 (2.1 × 50 mm) UPLC column (Waters Corp., Milford, MA, USA), maintained at 50 °C. Mass spectrometry detection was performed using a Xevo TQ mass spectrometer (Waters Corp., Milford, MA, USA) after electro-spray ionization in the positive ion mode with the following parameters: capillary voltage of 1.0 kV, desolvatation temperature at 450 °C, gas flow desolvatation at 850 L/h and gas flow cone at 50 L/h. Dry nitrogen (≥ 99.9%) was used as the desolvatation and nebulization gas, and argon (> 99.999%) was used as the collision gas (Air Liquid®, Paris, France). The multiple reaction monitoring modes were used. The parent ions and the suitable product ions (daughters) were selected: YSNSG 509.30 → 136.10 with a cone voltage = 30 V and energy collision = 30 eV; MRFA 524.40 → 104.10 with a cone voltage = 50 V and collision energy = 30 eV. The system control and data acquisition were performed using MassLynx® software (version 4.1; Waters Corp., Milford, MA, USA). The lower limit of quantification for YSNSG was fixed to 1 ng/mL with a coefficient of variation below 10%. The intra-assay precision and accuracy averaged 5.0% and 5.0%,

respectively. The inter-assay precision and accuracy averaged 11.0% and 11.0%, respectively, which is in line with FDA analytical recommendations.

2.13. Pharmacokinetic analysis

Finally, all the plasma and tissue parameters are measured between 0 and 2 hours. For the non-compartmental analysis, the concentration versus time data of YSNSG peptide were determined for each mouse by linear and nonlinear regression, considering the profiles of peptide concentrations in plasma using Prism® software (version 6.0; GraphPad Software, San Diego, California, USA) and MicroPharm-K (MicroPharm®, West Wales, UK). The choice of model describing the evolution of the concentration profiles of YSNSG was based on comparing the values of the Akaike information criterion (AIC). The median value of each interval was selected as the sampling time for each concentration measured. The exposure of the first and second intratumoral regions to YSNSG peptide from 0 to 2 hours was determined by the ratio of the areas under the curve in the extracellular fluid (ECF) in the central and peripheral regions (AUC_{ECF} / AUC_{plasma}), respectively. This ratio was considered to reflect the YSNSG peptide penetration into the tumor.

3. Results

All results are presented as average values ± standard deviation of the mean, unless otherwise stated.

3.1. Inhibition of *in vivo* tumor growth by the YSNSG peptide

The linear representation shown clear inhibition of tumor growth at D20 for the three groups treated with YSNSG (whatever the dose) contrary to control group (Fig. 2). At D24 the growth tumor inhibition seems to be attributable only to the YSNSG 20 mg/kg group. Based on LRT, AIC and BIC values, the model with only random effect on intercept (for each identity animal) was the most appropriate (Fig. 3). Nonlinear evolutions, using restricted

cubic splines, improved the model fitting (LRT p <0.0001; ΔAIC = 7; ΔBIC = 11). No residual weighting was required. The integration of the group covariate improved significantly the model (LRT p <0.0001; ΔAIC = 30; ΔBIC = 22). As the control group was taken as reference, all parameter estimate of treatment (20, 10, 5 mg/kg) was considered as the coefficient indicating the effect of the treatment compared to the control. Difference of the coefficient with zero value were checked with Wald test and Confidence Interval [%95CI] which was estimated using non-parametric bootstrapping (n-simulations=1000). The mixed effect model of tumor growth was validated for: good correlation between observed and predicted individual measures (r^2 = 0.75, p <0.0001), normal distribution of pearson residuals which were centred on zero without systematic bias. Estimated model parameters are presented in Table 1. All the estimated parameter were confirmed using bootstrapping procedure (n=1000). Compared to the control group, the model indicated that 20 mg/kg of YSNSG peptide inhibits significantly tumor growth (20 mg/kg vs Control [(T_{vol})/day]: coefficient = -143.73657, -264.94690; -22.52625], p=0.022). Based on these results, the dose for pharmacokinetic experimentation has been 20 mg/kg.

3.2.*In vitro and in vivo* relative recoveries and plasma protein binding

The relative recovery of the microdialysis probe of YSNSG peptide was 69.7 ± 4.5%. The relative recoveries of the microdialysis probes of YSNSG peptide in mice using the reverse dialysis method were 79.3 ± 6.6% in the region 1 of the tumor and 79.1 ± 7.4% in the region 2 of the tumor, respectively. All dialysates values shown in the *Results* were corrected according to the relative recoveries of both microdialysis probes. Plasma protein binding (PPB) was determined at 42.6 ± 11.4% and, similarly, plasma values were corrected accordingly.

3.3.YSNSG pharmacokinetic with non-compartmental analysis

The concentration-time profile of YSNSG in plasma showed a monocompartmental decrease with an elimination half-life of 25.8 ± 8.2 min, a volume of distribution of 11.9 ± 0.4 mL, a total clearance of 19.8 ± 9.4 mL/h and a median residence time (MRT) of 0.62 ± 0.2 h. The area under the curve (AUC) from 0 to 2 hours was 1,173.6 ± 556.3 µg.min/mL (Table 2 and Fig. 4) and the extrapolated AUC was of 3,4%. The evolution of intratumoral disposition of YSNSG peptide showed similar pharmacokinetic profiles with a C_{max} of 406.7 ± 207.6 ng/mL in the region 1 and 390.3 ± 324.3 ng/mL in the region 2, respectively. The T_{max} interval (depending to the frequency of dialysate collections) has been found between 30 and 60 min for region 1 whereas it has been found between 60 and 90 min for region 2 of the tumor. Finally the drug penetration into the tumor (AUC_{ECF}/AUC_{plasma} ratio) was 3.3 ± 2.1% for region 1 and 3.4 ± 2.7% for region 2 of the tumor, respectively.

4. Discussion

Pharmacological activity of any drug results in a sufficient quantity of active (unbound) drug in the extracellular fluid close to the biological target. The quantity of drug in the extracellular fluid is associated to drug tissue disposition from plasma compartment. For antineoplastic this requires the transport of drugs from intratumoral blood vessels to extracellular fluid at the border of the tumor cells. In this way YSNSG peptide has to bind $\alpha_v\beta_3$ integrin on tumor cell surface to prevent their adhesion to the basement membrane (Thevenard et al., 2006). Only one dose has been assessed in biological study as well as in pharmacokinetic study (Thevenard et al., 2006 ; Slimano et al., 2017). However, *in vitro* studies showed a dose-effect for cell proliferation inhibition, the pro-MMP-2 activation cascade inhibition and the plasminogen activator secretion inhibition (Thevenard et al., 2006). In order to enhance drug disposition into in vivo tissues, we had to re-explore the dose-effect of YSNSG peptide in a melanoma model using multiple doses and measuring tumor growth inhibition. When the statistical analysis on repeated measures showed no significant differences between doses, the

use of a mixed model effect showed a statistical significant difference between 20 mg/kg and lower doses in term of growth tumor inhibition. The use of a mixed model effect in this biologic context should be supported by the fact that it uses long data format and includes fixed and random effects for which it can provide correct standard errors. Compared to analysis of variance (ANOVA), mixed effects models present advantages for developmental studies (Wainwright et al., 2007).

After identifying a dose of 20 mg/kg as having significantly greater effects than 10 mg/kg we investigate the intratumoral disposition of YSNSG peptide. Considering microdialysis parameters, the relative recovery appears to be high but consistent with literature taking into account the same flow rate (Plock and Kloft, 2005). Moreover, the relative recovery was approximately the same between both investigated intratumoral regions, supporting the value of using this method. However, we do not investigated the hypothesis of YSNSG peptide binding in non-specific site of microdialysis tubing and the possible consequence on relative recovery values, as detailed in previous studies relative to microdialysis of monoclonal antibodies (Jadhav et al., 2017 ; Chang et al., 2018).

Considering plasma parameters, the volume of distribution is high and in accordance with an important tissue disposition of YSNSG peptide as previously described in rat (Slimano et al., 2017). Indeed in our previous study Vd was 433 mL for Wistar rats (weighing 250 g) for which the blood volume was estimated to 16 mL (Lee and Blaufox, 1985) and consequently a ratio Vd / blood volume approximately of 27. When taking into account the blood volume per 100 g for mouse (approximately 9 mL/100 g) (Riches et al., 1973) and considering mouse of 20 g the blood volume can be assessed at 0.2 mL approximately. In our study we found a Vd of 6.9 mL and a ratio Vd / blood volume of 35, in the same order as rats. For other main plasma parameters e.g. elimination half-life (25.8 min), total clearance (19.8 mL/h) and area under the curve (1,173,559 ng.min/mL), there was not possible to directly compare to Wistar

rats plasma parameters. Another reason of the non-comparison is the difference in the follow up time of both animal species. In our first study, Wistar rats were followed during 5 hours whereas in this study we follow up mice during 2 hours because of the difficulty of collecting several blood samples in this animal model. This can introduce a misestimating of pharmacokinetics parameters.

When plasma and tissue parameters are analyzed together, there are two main comments to make: first we found that drug penetration are low in comparison with subcutaneous distribution of YSNSG peptide from the previous study in rats, and secondly we found no heterogeneity between the two measure points into the tumor which seems to relfect a possible relative homogeneity in the intratumoral disposition of YSNSG peptide.

First, the AUC_{ECF}/AUC_{plasma} ratios were 3.3 ± 2.1% for central region and 3.4 ± 2.7% for peripheral region of the tumor, respectively. This intratumoral penetration appears to be low compared to the previous study in healthy Wistar rats where YSNSG peptide penetration was assessed to 66.2 ± 21.6% in a subcutaneous tissue (Slimano et al., 2017). When we designed the study we hypothesized that intratumoral tissue would be comparable in term of pharmacokinetics to a superficial tissue compartment as well as subcutaneous tissue but our results showed that intratumoral tissue seems to be much closer than cerebral drug penetration of YSNSG peptide (3.6 ± 4.7%) which is considered as a deep tissue compartment. However, and contrary to drug penetration in cerebral tissue which appears to be consistently low, the drug penetration into the tumor is unpredictable. In a preclinical study using rats, carcinosarcoma W-256 and etoposide, the AUC ratios were approximately 30% in central region and 60% in peripheral region of the tumor, respectively (Pigatto et al., 2016). In another study using eribulin in a xenograft mice model the disposition in tumor (determined without using microdialysis) was considerable, 17-23 fold higher than in plasma (Sugawara et al., 2017). The major differences can be related to the type of tumor but maybe also to the

drug used. About the tumor influence, the drug diffusion from intratumoral blood vessels to extracellular fluid is related to concentrations gradient. Consequently it can be influenced by the oncotic pressure gradient known in tumors to be almost zero and the interstitial fluid pressure which is often elevated and approximately the same as the microvascular pressure (Netti et al., 1999 ; Stohrer et al., 2000). In the same way, high interstitial fluid pressure has been associated with poor drug penetration (Heldin et al., 2004). Moreover, the composition and the organization of the extracellular matrix and the tumor cell architecture can also affect drug penetration (Davies et al., 2002). About the drug influence, for example in cerebral tissue several studies found a penetration rate range from 2.5% to 7.4% for methotrexate (Devineni, Klein-Szanto and Gallo, 1996 ; Dukic et al., 2004) whereas one study showed a penetration rate of 18.6% for gemcitabine in the same tumor model than for methotrexate (Apparaju, Gudelsky and Desai, 2008). In clinical studies using microdialysis the penetration rate in subcutaneous tumors was assessed for 5-fluorouracile from 17% to 41% and for carboplatine from 64% to 100%, respectively (Koning et al., 2009 ; Konings et al., 2011).

Secondly, our study showed relative intratumoral homogeneity in the disposition of YSNSG peptide between two different points into the tumor, as well as the same relative recovery. These results are in contradiction with the documented knowledges supporting the concept of tumor heterogeneity and their consequences on the disposition of antineoplastic (Trédan et al., 2007 ; Tannock et al., 2002 ; Grantab and Tannock, 2012). Numerous factors are associated with these intratumoral interferences: first the nutrition deprivation occurring on the central region of tumor can lead to a decrease of tumor cells proliferation in correlation with the increasing distance from intratumoral vessels (Tannock, 1968 ; Hisrt and Denekamp, 1979). It results in a less effective activity of antineoplastic because of a majority of quiescent cells instead of proliferating cells (Tannock, 1978). Secondly and in relation to intratumoral deprivation, tumor hypoxia can induce the activation of genes that are associated with

angiogenesis and cell survival with the mediation of Hypoxemia-Inductible Factor-1 (Pouysségur, Dayan and Mazure, 2006). This can lead to the proliferation of cells with altered biochemical pathways that may have a drug-resistant phenotype (Trédan et al., 2007). Finally sequestration of drugs in tumor cells can inhibit drug penetration to deeper regions of the tumor (Berk et al., 1997). Conversely, drug diffusion can also be influenced by elimination half-life because high half-life will give a more uniform disposition even if its extravasation and penetration of tissues are relatively slow, whereas a drug that has a short half-life will have a non-uniform disposition (Trédan et al., 2007). This can explain, at least in part, the uniform YSNSG peptide disposition in our study regarding the half-life and the tumor volume similar to clinical studies (Koning et al., 2009 ; Konings et al., 2011). An experimental explanation can also be related to the length of microdialysis probes we used.

In this study we used a length of 10 mm and, taking into account the average tumor size, we cannot exclude that regions 1 and 2 haven't been sufficiently separated and could probably explain the non-difference of AUC ratio between both intratumoral regions. We chose a 10-mm probe length to minimize the hypothetical risk of analytical difficulties with probes length of 4 mm but we are aware that it was maybe not justified regarding the low LLOQ of YSNSG peptide. The study of Pigatto et al. also uses length probes of 10 mm and was able to find heterogeneous intratumoral disposition of etoposide (Pigatto et al., 2016), even if the average tumor volume in this study was around 5 cm^3 whereas this average tumor volume in our study ranged around 2.5 cm^3.

5. Conclusions

As well as our previous pharmacokinetic study, this study is the first to investigate intratumoral disposition of the YSNSG peptide. This is of major way to continue development of this integrin antagonist against melanoma. The low intratumoral penetration rate described

should be considered to an opportunity for pharmaceutical modulation as nanoencapsulation. Different approaches of YSNSG peptide encapsulation are currently under investigation in order to enhance intratumoral penetration of the YSNSG peptide.

Acknowledgements

This work has awarded a joint research grant from Académie Nationale de Pharmacie (« Elie Bzoura » grant) and Société Française de Pharmacie Oncologique (SFPO).

This work was supported by grants from the Centre National de la Recherche Scientifique (UMR 7369), the University of Reims Champagne-Ardenne, and the Conférence de Coordination Interrégionale de la Ligue Contre le Cancer du Grand Est (CCIR-GE).

References

Apparaju, S.K., Gudelsky, G.A., Desai, P.B., 2008. Pharmacokinetics of gemcitabine in tumor and non-tumor extracellular fluid of brain: an in vivo assessment in rats employing intracerebral microdialysis. Cancer Chemother. Pharmacol. 61, 223‑229. DOI: 10.1007/s00280-007-0464-1.

Bates, D., Maechler, M., Bolker, B., Walker, S., 2015. Fitting linear mixed-effects models using lme4. J. Stat. Soft. 67, 1-48. DOI: 10.18637/jss.v067.i01.

Berk, D.A., Yuan, F., Leunig, M., Jain, R.K., 1997. Direct in vivo measurement of targeted binding in a human tumor xenograft. Proc. Natl. Acad. Sci. 94, 1785‑1790. DOI: 10.1073/pnas.94.5.1785.

Chang, H.Y., Morrow, K., Bonacquisti, E., Zhang, W., Shah, K., 2018. Antibody pharmacokinetic in rat brain determined using microdialysis. MAbs 10, 843-853. DOI: 10.1080/19420862.2018.1473910.

Davies, C de L., Berk, D.A., Pluen, A., Jain, R.K., 2002. Comparison of IgG diffusion and extracellular matrix composition in rhabdomyosarcomas grown in mice versus in vitro as spheroids reveals the role of host stromal cells. Br. J. Cancer 86, 1639‑1644. DOI: 10.1038/sj.bjc.6600270.

Devineni, D., Klein-Szanto, A., Gallo, J.M., 1996. In vivo microdialysis to characterize drug transport in brain tumors: analysis of methotrexate uptake in rat glioma-2 (RG-2)-bearing rats. Cancer Chemother. Pharmacol. 38, 499‑507. DOI: 10.1007/s002800050518.

Djerada, Z., Feliu, C., Cazaubon, Y., Smati, F., Gomis, P., Guerrot, P., et al., 2017. Population Pharmacokinetic-Pharmacodynamic Modeling of Ropivacaine in Spinal Anesthesia. Clin Pharmacokinet. 57, 1135-1147. DOI: 10.1007/s40262-017-0617-2.

Djerada, Z., Feliu, C., Tournois, C., Vautier, D., Binet, L., Robinet, A., et al., 2013. Validation of a fast method for quantitative analysis of elvitegravir, raltegravir, maraviroc, etravirine, tenofovir, boceprevir and 10 other antiretroviral agents in human plasma samples with a new UPLC-MS/MS technology. J. Pharm. Biomed. Anal. 86, 100-111. DOI: 10.1016/j.jpba.2013.08.002.

Dukic SF, Kaltenbach ML, Heurtaux T, Hoizey G, Lallemand A, Vistelle R. Influence of C6 and CNS1 brain tumors on methotrexate pharmacokinetics in plasma and brain tissue. *J Neurooncol* 2004; 67(1‑2):131‑8. DOI: 10.1023/B:NEON.0000021820.12444.4c.

Francavilla, C., Maddaluno, L., Cavallaro, U., 2009. The functional role of cell adhesion molecules in tumor angiogenesis. Semin Cancer Biol. 19, 298‑309. DOI: 10.1016/j.semcancer.2009.05.004.

Grantab, R.H., Tannock, I.F., 2012. Penetration of anticancer drugs through tumour tissue as a function of cellular packing density and interstitial fluid pressure and its modification by bortezomib. BMC Cancer 12, 214. DOI: 10.1186/1471-2407-12-214.

Hanahan, D., Weinberg, R.A., 2011. Hallmarks of cancer: the next generation. Cell 144, 646-674. DOI: 10.1016/j.cell.2011.02.013.

Heldin, C.H., Rubin, K., Pietras, K., Ostman, A., 2004. High interstitial fluid pressure - an obstacle in cancer therapy. Nat. Rev. Cancer 4, 806‑813. DOI: 10.1038/nrc1456.

Hirst, D.G., Denekamp, J., 1979. Tumour cell proliferation in relation to the vasculature. Cell Tissue Kinet. 12, 31‑42. DOI: 10.1111/j.1365-2184.1979.tb00111.x.

Konings IRHM, Engels FK, Sleijfer S, Verweij J, Wiemer EAC, Loos WJ., 2009. Application of prolonged microdialysis sampling in carboplatin-treated cancer patients. Cancer Chemother. Pharmacol. 64, 509‑516. DOI: 10.1007/s00280-008-0898-0.

Konings, I.R.H.M., Sleijfer, S., Mathijssen, R.H.J., de Bruijn, P., Ghobadi Moghaddam-Helmantel, I.M., van Dam, L.M,, et al., 2011. Increasing tumoral 5-fluorouracil concentrations during a 5-day continuous infusion: a microdialysis study. Cancer Chemother. Pharmacol. 67(5):1055‑62. DOI: 10.1007/s00280-010-1400-3.

Netti, P.A., Hamberg, L.M., Babich, J.W., Kierstead, D., Graham, W., Hunter, G.J., et al., 1999. Enhancement of fluid filtration across tumor vessels: Implication for delivery of macromolecules. Proc. Natl. Acad. Sci. 96, 3137‑3142. DOI: 10.1073/pnas.96.6.3137.

Pigatto, M.C., de Araujo, B.V., Torres, B.G.S., Schmidt, S., Magni, P., Dalla Costa, T., 2016. Population Pharmacokinetic Modeling of Etoposide Free Concentrations in Solid Tumor. Pharm. Res. 33, 1657‑1670. DOI: 10.1007/s11095-016-1906-4.

Plock, N., Kloft, C., 2005. Microdialysis—theoretical background and recent implementation in applied life-sciences. Eur. J. Pharm. Sci. 5, 1‑24. DOI: 10.1016/j.ejps.2005.01.017.

Pouysségur, J., Dayan, F., Mazure, N.M., 2006. Hypoxia signalling in cancer and approaches to enforce tumour regression. Nature 441, 437‑443. DOI: 10.1038/nature04871.

Riches, A.C., Sharp, J.G., Thomas, D.B., Smith, S.V., 1973. Blood volume determination in the mouse. J. Physiol. 228, 279‑284. DOI: 10.1113/jphysiol.1973.sp010086.

Scheller, D., Kolb, J., 1991. The internal reference technique in microdialysis: A practical approach to monitoring dialysis efficiency and to calculating tissue concentration from dialysate samples. J. Neurosci. Methods 40, 31‑38. DOI: 10.1016/0165-0270(91)90114-F.

Shattil, S.J., Kim, C., Ginsberg, M.H., 2010. The final steps of integrin activation: the end game. Nat. Rev. Mol. Cell Biol. 11, 288‑300. DOI: 10.1038/nrm2871.

Slimano, F., Djerada, Z., Bouchene, S., Van Gulick, L., Brassart-Pasco, S., Dukic, S., 2017. First plasma and tissue pharmacokinetic study of the YSNSG cyclopeptide, a new integrin antagonist, using microdialysis. Eur. J. Pharm. Sci. 105, 178‑87. DOI: 10.1016/j.ejps.2017.05.016.

Ståhle, L., Arner, P., Ungerstedt, U., 1991. Drug distribution studies with microdialysis. III: Extracellular concentration of caffeine in adipose tissue in man. Life Sci. 49, 1853‑1858. DOI: 10.1016/0024-3205(91)90488-w.

Stohrer, M., Boucher, Y., Stangassinger, M., Jain, R.K., 2000. Oncotic pressure in solid tumors is elevated. Cancer Res. 60, 4251‑4255.

Sugawara, M., Condon, K., Liang, E., DesJardins, C., Schuck, E., Kusano, K., et al., 2017. Eribulin shows high concentration and long retention in xenograft tumor tissues. Cancer Chemother. Pharmacol. 80, 377‑384. DOI: 10.1007/s00280-017-3369-7.

Tannock, I., 1978. Cell kinetics and chemotherapy: a critical review. Cancer. Treat. Rep. 62, 1117‑1133.

Tannock, I.F., 1968. The relation between cell proliferation and the vascular system in a transplanted mouse mammary tumour. Br. J. Cancer 22, 258‑273. DOI: 10.1038/bjc.1968.34.

Tannock, I.F., Lee, C.M., Tunggal, J.K., Cowan, D.S.M., Egorin, M.J., 2002. Limited penetration of anticancer drugs through tumor tissue: a potential cause of resistance of solid tumors to chemotherapy. Clin. Cancer Res. 8, 878‑884.

Thevenard, J., Floquet, N., Ramont, L., Prost, E., Nuzillard, J.-M., Dauchez, M., et al., 2006. Structural and Antitumor Properties of the YSNSG Cyclopeptide Derived from Tumstatin. Chem. Biol. 13, 1307‑1315. DOI: 10.1016/j.chembiol.2006.10.007.

Thevenard, J., Ramont, L., Devy, J., Brassart, B., Dupont-Deshorgue, A., Floquet, N., et al., 2010. The YSNSG cyclopeptide derived from tumstatin inhibits tumor angiogenesis by down-regulating endothelial cell migration. Int. J. Cancer 126, 1055–1066. DOI: 10.1002/ijc.24688.

Trédan, O., Galmarini, C.M., Patel, K., Tannock, I.F., 2007. Drug resistance and the solid tumor microenvironment. J. Natl. Cancer Inst. 99, 1441‑1454. DOI: 10.1093/jnci/djm135.

Wainwright, P.E., Leatherdale, S.T., Dubin, J.A., 2007. Advantages of mixed effects models over traditional ANOVA models in developmental studies: a worked example in a mouse model of fetal alcohol syndrome. Dev. Psychobiol. 49, 664‑674. DOI: 10.1002/dev.20245

Wald, M., Olejár, T., Sebková, V., Zadinová, M., Boubelík, M., Poucková, P., 2001. Mixture of trypsin, chymotrypsin and papain reduces formation of metastases and extends survival time of C57Bl6 mice with syngeneic melanoma B16. Cancer Chemother. Pharmacol. 47 Suppl, S16-22. DOI: 10.1007/s002800170004.

Yardeni, T., Eckhaus, M., Morris, H.D., Huizing, M., Hoogstraten-Miller, S., 2011. Retro-orbital injections in mice. Lab. Anim. 40, 155‑160. DOI: 10.1038/laban0511-155.

Figures and Tables

Figure 1: Pictoral representation of the microdialysis probes insertion into B16F1 melanoma tumor. Adapted by permission from Springer Nature: Pharmaceutical Research: Population Pharmacokinetic Modeling of Etoposide Free Concentrations in Solid Tumor, MC Pigatto, COPYRIGHT n°4516100344084, 2016.

Figure 2: Graphical illustration of tumor growth inhibition by YSNSG peptide after administration of 5 mg/kg (blue), 10mg/kg (orange), 20 mg/kg (green) or control (pink line). Error bars are Standard Deviation.

Figure 3: Illustration of the mixed effect model of tumor growth inhibition by YSNSG peptide 5 mg/kg (blue), 10mg/kg (orange), 20 mg/kg (green) or control (pink line).

Figure 4: Graphical illustration of the concentration-time evolution of YSNSG peptide in plasma and tissues (central and peripheral region of melanoma tumor). Error bars are Standard Deviation.

Table 1: Non-linear mixed effect model of tumor growth inhibition by YSNSG peptide after administration of 5 mg/kg, 10mg/kg, 20 mg/kg or control (n=10 in each group).

Table 2: Plasma and intratumoral pharmacokinetic of YSNSG peptide in B16F1 melanoma mice (n=8).

Supplementary file 1: Photography of a anesthetized tumor-bearing (B16F1) mouse (C57Bl/6) with insertion of the two microdialysis probes into the different intratumoral regions. Microdialysis probes were CMA/20 with a membrane lenght of 10 mm and a cutoff of 20 kDa.

Supplementary file 2: Diagnostic plot. Model validation of non-linear mixed effect model of tumor growth inhibition by YSNSG peptide. a: Regression or correlation between observed and predicted values (Tvol); b: Pearson residuals as function of feeted data; c: QQplot of residuals; d: Histogram of residuals.

Table 1: Non-linear mixed effect model of tumor growth inhibition by YSNSG peptide after administration of 5 mg/kg, 10 mg/kg, 20 mg/kg or control (n=10 in each group).

Parameters	**Estimate**	**Standard Error**	**IC [%95CI]***	**Wald test p value**
Intercept	51.9458	59.99495	[-64.78048 ; 168.67209]	0.3875
ns(**Time** [days], 3) first level of spline	1229.1832	113.57142	[1008.21848 ; 1450.14800]	0
ns(**Time** [days], 3) second level of spline	1822.9048	78.29194	[1670.57988 ; 1975.22977]	0
20 mg/kg vs Control [(Tvol)/day]	-143.73657	62.29966	[-264.94690 ; -22.52625]	0.022
10 mg/kg vs Control [(Tvol)/day]	32.4924	65.19260	[94.34643 ; 159.33126]	0.6187
5 mg/kg vs Control [(Tvol)/day]	-45.77138	65.16682	[-172.56008 ; 81.01731]	0.4832
Within group standard error	344.6336	0.03571023	[314.9638 ; 377.0983]	-

*95 % confidence interval calculated using parametric bootstrapping (n-simulations=1000); ns: natural cubic splines

Table 2: Plasma and intratumoral pharmacokinetic of YSNSG peptide in B16F1 melanoma mice (n=8).

Plasma* pharmacokinetic parameters	**Mean ± SD**
Dose (ng)	512,500 ± 35,355
C_{max} (ng/mL)	44,971 ± 7,948
λ (min^{-1})	0.030 ± 0.011
$T_{1/2}$ (min)	25.8 ± 8.2
Vd (mL)	11.9 ± 0.4
AUC (ng.min/mL)	1,173,559 ± 556,255
AUC extrapolated (%)	3.4
Total clearance (mL/h)	19.8 ± 9.4
MRT (h)	0.62 ± 0.2
Intratumoral pharmacokinetic parameters	
Region 1 C_{max} (ng/mL)	406.7 ± 207.6
Region 2 C_{max} (ng/mL)	390.3 ± 324.3
Region 1 AUC (ng.min/mL)	31,636 ± 11,160
Region 2 AUC (ng.min/mL)	31,912 ± 16,756
Region 1 AUC_{ECF} / AUC_{plasma} ratio (%)	3.3 ± 2.1
Region 2 AUC_{ECF} / AUC_{plasma} ratio (%)	3.4 ± 2.7

*All plasma parameters were corrected by the Plasma Protein Binding; SD: Standard Deviation; C_{max}: maximal concentration; λ: elimination rate constant; $T_{1/2}$: half-life elimination; V_d: Volume of distribution; AUC: Area Under the Curve; ECF: Extracellular Fluid; MRT: Mean Residence Time

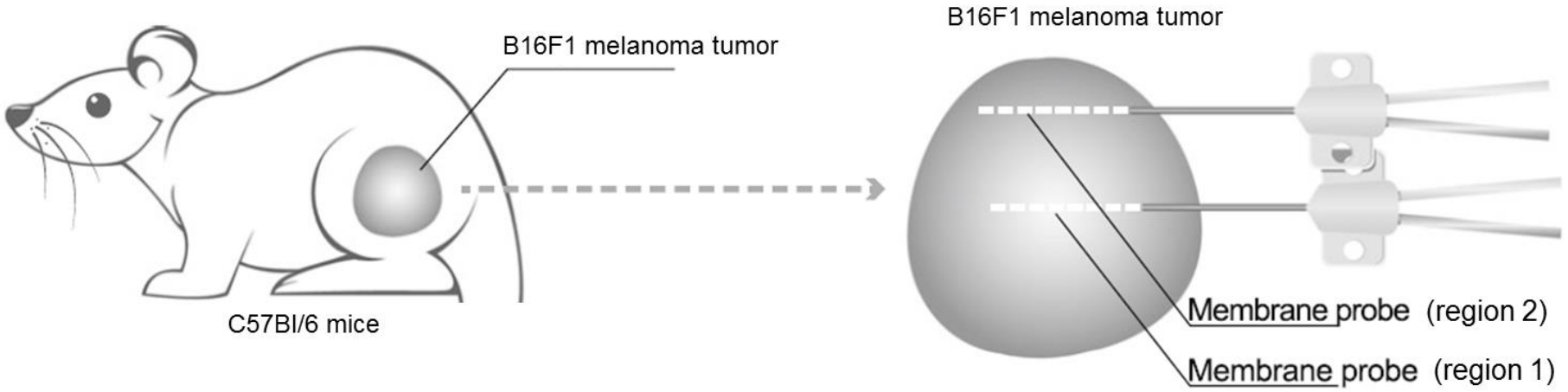

Figure 1: Pictoral representation of the microdialysis probes insertion into B16F1 melanoma tumor. Adapted by permission from Springer Nature: Pharmaceutical Research: Population Pharmacokinetic Modeling of Etoposide Free Concentrations in Solid Tumor, MC Pigatto, COPYRIGHT n°4516100344084, 2016.

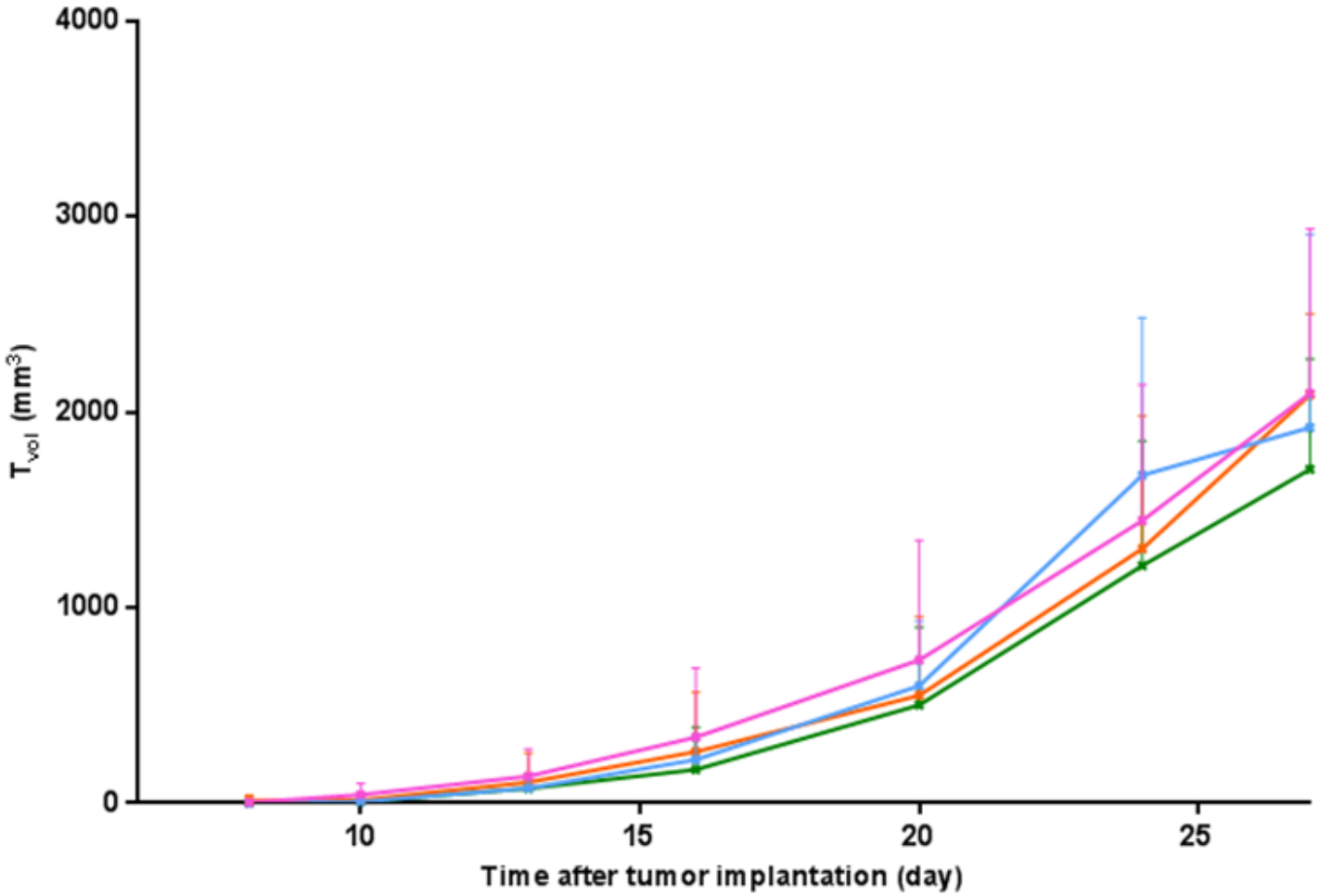

Figure 2: Graphical illustration of tumor growth inhibition by YSNSG peptide after administration of 5 mg/kg (blue), 10mg/kg (orange), 20 mg/kg (green) or control (pink line). Error bars are Standard Deviation.

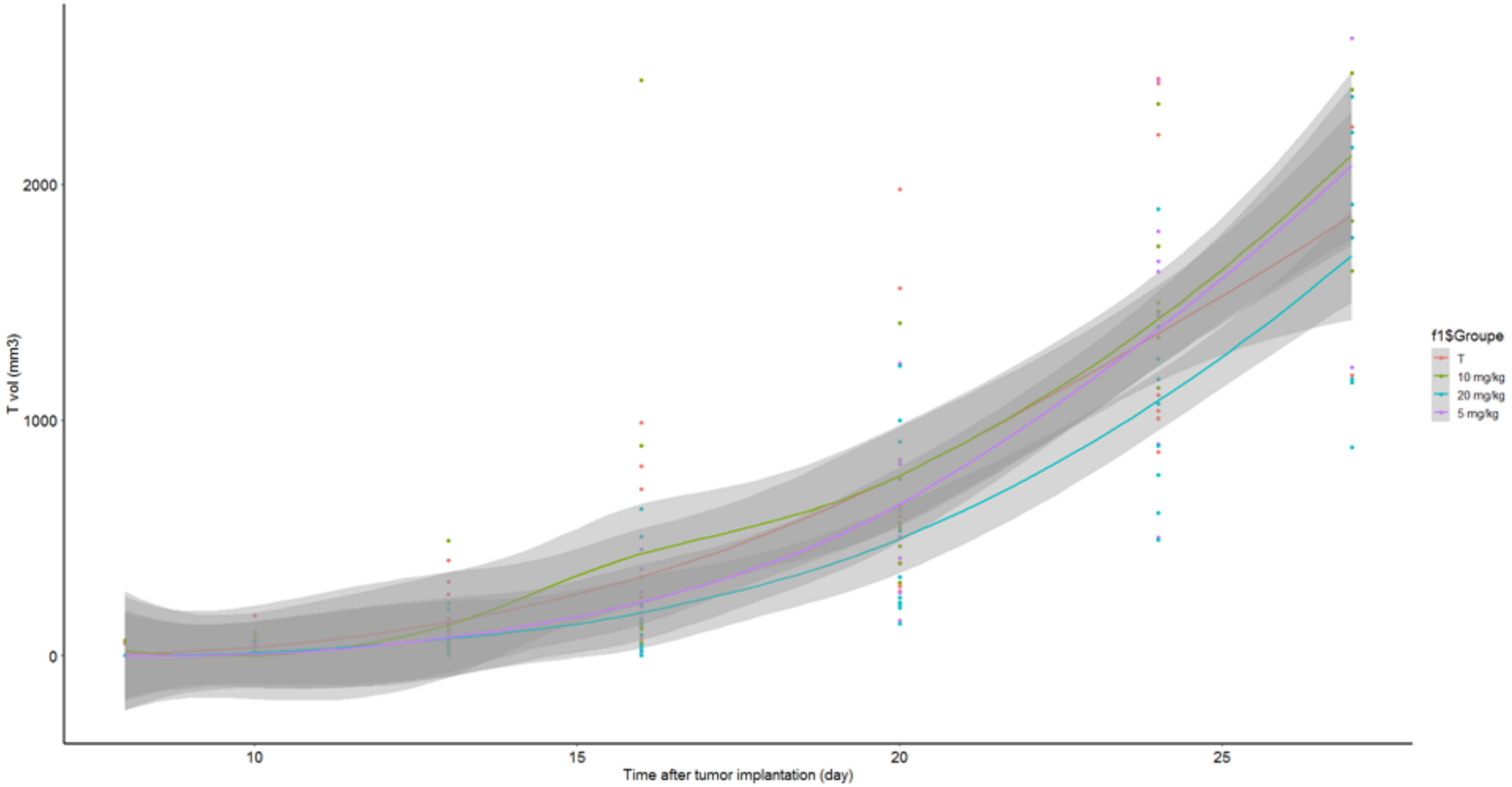

Figure 3: Illustration of the mixed effect model of tumor growth inhibition by YSNSG peptide 5 mg/kg (blue), 10mg/kg (orange), 20 mg/kg (green) or control (pink line).

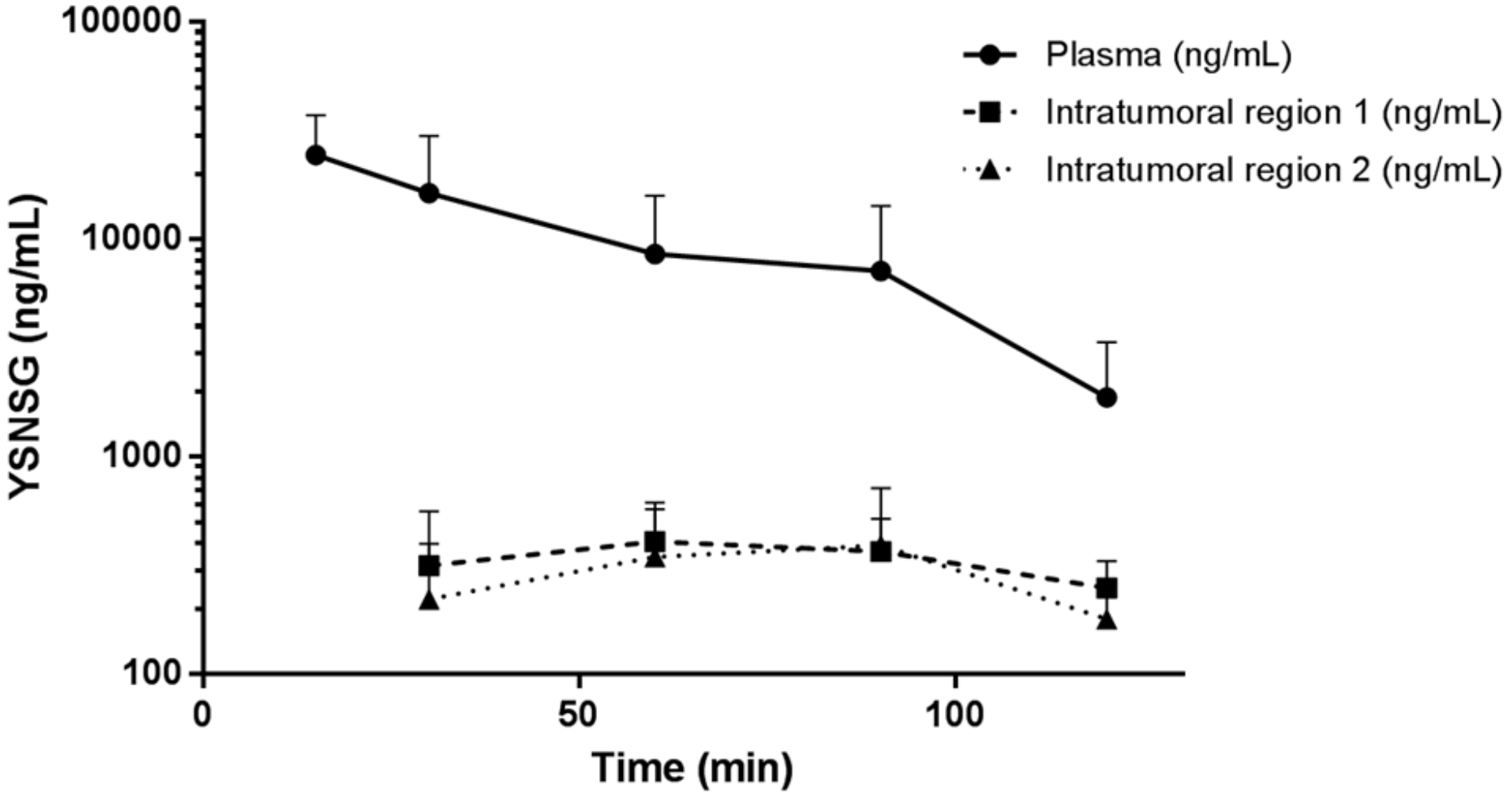

Figure 4: Graphical illustration of the concentration-time evolution of YSNSG peptide in plasma and tissues (central and peripheral region of melanoma tumor). Error bars are Standard Deviation.